Fluid flow at the center of a cross composed of tubes

T. A. Fox and N. Toy
Department of Civil Engineering, University of Surrey, Guildford, Surrey, GU2 5XH, UK

Received 16 May 1986 and accepted for publication 27 May 1987

This paper presents details of an experimental investigation designed to determine the flow regimes associated with two tubes arranged in the geometry of a cross. Consideration has been given to the effect of tube spacing upon the fluid motion at the center of the configuration, and comments are made on the possible heat transfer implications of this work. Two fundamental flow patterns were found, which are related to a critical tube spacing. When the distance separating the tubes is less than three diameters, $L < 3D$, two stationary recirculation cells are present in the gap formed at the center of the cross, whereas at spacings beyond three diameters, $L > 3D$, these cells are replaced by vortex shedding in the wake of the central portion of the upstream tube. It is suggested that these flow regimes may lead to increased heat transfer rates at the surface of the downstream tube, particularly within a spanwise region of two and a half diameters from the center of the cross.

Keywords: cylinder; fluid flow; heat transfer; tubes

Introduction

Thermal cooling systems used in the power generation industry employ heat exchangers which are often composed of tube arrays arranged in various configurations to a flow of coolant. For instance, the tubes may be set in rows perpendicular or parallel to the direction of the free-stream or, alternatively, as a series of grids with each element orientated at 90° to that preceding it. Since it is well known that the heat transfer process at the surface of a tube is dependent upon the fluid motion in the approach flow, Van der Hegge Zijnen,[1] the structure of the turbulence developed in these arrangements is of considerable importance to the design and analysis of the associated thermohydraulic mechanisms.

Several studies have considered the fluid motion in heat exchangers composed of tubes set in rows normal to the approach flow, and many of these have been summarized in a review paper presented by Zdravkovich.[2] In this field fundamental work has been carried out by Kostic and Oka[3] involving the use of two cylinders in tandem to simulate the flow conditions within "in-line" tube banks. The complementary case of rows aligned axially to the free-stream was examined recently by Hooper and Rehme,[4] among others. However, there remains considerable scope for an investigation of the relationship between fluid flow and heat transfer with regard to tubes arranged in grid configurations.

A grid formation of this type can be regarded in its simplest form as a single node composed of two tubes perpendicular to each other in the geometry of a cross. Such a configuration in itself produces a flow field which, at the present, is not amenable to a detailed theoretical analysis, and, consequently, the main approach to this problem involves the use of experimental techniques. However, due to the highly complex nature of the fluid motion and the difficulty in measuring the associated parameters, very few studies have been carried out in this area.

A limited number of investigations have been undertaken recently to examine the flow phenomena produced by perpendicular cylinders that intersect in a single plane, notably by Osaka *et al.*[5-7] and Zdravkovich.[8] Zdravkovich[9] has also determined limited details of the interference to flow caused by two cylinders placed one behind the other to form a cross with the members in contact at the center. Consideration has not, however, been given to the fluid motion associated with the flow around nonconnecting cylinders displaced relative to each other in the direction of the free stream. This paper, therefore, discusses the results of experimental work designed to determine the fluid behavior at the center of such a cross.

Experimental arrangement

The experimental investigation was carried-out in a low-speed, blow-down, open-circuit wind tunnel with working section dimensions of width 1.067 m, height 1.372 m, and length 9.0 m, as illustrated in Figure 1. This produces a uniform airflow with a free-stream turbulence intensity of approximately 0.17% at the model testing position.

A pair of 30-mm diameter aluminum tubes formed the cross, which completely spanned the working section in the vertical and horizontal directions. Each tube was polished to a smooth finish to avoid a change in the effective Reynolds number as a result of surface roughness, E.S.D.U. 80025.[10] The vertical tube could be displaced in the direction of the free-stream flow to produce a gap at the center of the configuration. The coordinate system based on this geometry is shown in Figure 2, which also defines the separation distance, L. The blockage percentage associated with each tube was calculated in accordance with E.S.D.U. 80024[11] and was found to be 2.2% and 2.8% for the horizontal and vertical models, respectively. It was therefore considered unnecessary to apply a correlation factor to the experimental data.

Mean surface pressure distributions were measured by the use of 0.5-mm-diameter tappings arranged around the centerline of the model. These were connected to a low-pressure transducer via a Scanivalve switch mechanism. The latter was controlled by a Commodore microcomputer, which also performed data acquisition and on-line analysis as described in Savory and Toy.[12] The free-stream reference pressure was obtained from a pitot-static tube positioned in the uniform flow. Values of the coefficient of pressure, C_p, were calculated directly for each location by the use of this method and in accordance with the

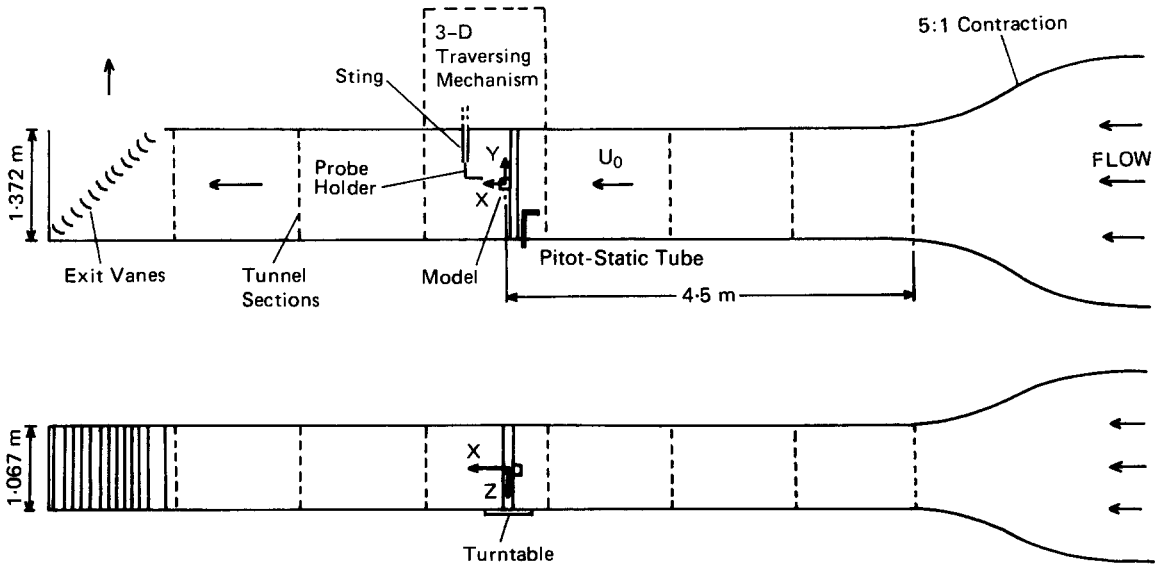

Figure 1 Diagrammatic layout of 1.067 m × 1.372 m × 9.0 m wind tunnel

expression

$$C_p = \frac{P_L - P_0}{\frac{1}{2}\rho U_0^2}$$

where P_L is the local surface pressure, P_0 is the free-stream static pressure, and $\frac{1}{2}\rho U_0^2$ is the dynamic head of the free-stream. This system produced values of C_p from the mean of 30,000 samples with a repeatable accuracy of 1.5%.

Velocity and turbulence intensity data were obtained with a pulsed wire anemometer. This instrument is appropriate for use in highly turbulent flow and was of a type similar to that described by Bradbury and Castro.[13] Movement of the anemometer within the flow field was achieved by mounting the probe on the "sting" of a precision three-dimensional traversing system, which has a positional accuracy of ±0.02 mm. On-line data acquisition and analysis was performed by the Commodore microcomputer, and each result was calculated from the mean of 5000 samples.

Spatial correlation coefficients were determined from u-component fluid velocities measured by the use of two constant temperature single hot wire anemometers. These were P11 type probes and were used in conjunction with DISA 55M10 units. One of the anemometers was positioned at a selected point in the flow field under consideration and remained stationary while the other was attached to the sting of the traversing mechanism for movement to locations at which correlation was required.

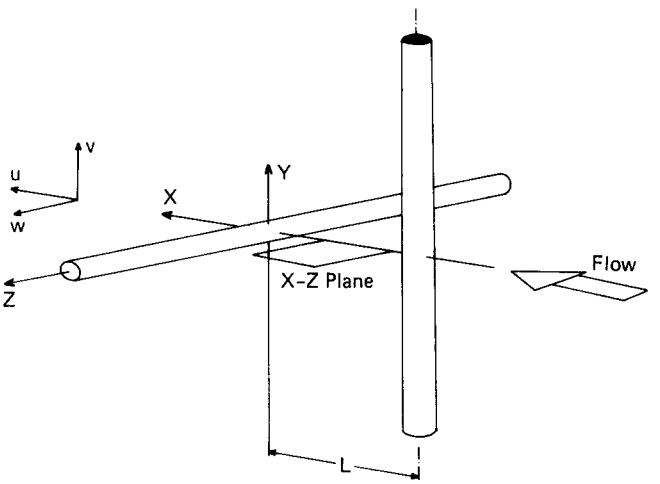

Figure 2 Model geometry and coordinate system

Notation

C_p	Pressure coefficient, $(P_L - P_0)/\frac{1}{2}\rho U_0^2$
C_{pb}	Pressure coefficient measured on the base centerline
C_{ps}	Pressure coefficient measured at the stagnation point
$C_{p(min)}$	Minimum pressure coefficient
D	Diameter of tube
L	Distance between central axis of each tube
L_{uz}	Integral length scale in Z-direction, $\int_0^z R_u(Z)\,dz$
P_L	Local pressure on model's surface
P_0	Static pressure
P_T	Free-stream total pressure
R_u	Spatial correlation coefficient, $\frac{\overline{u_1' \times u_2'}}{\sqrt{\overline{u_1'^2}} \times \sqrt{\overline{u_2'^2}}}$
Re	Reynolds number, DU_0/ν
U_0	Mean free-stream velocity in X-direction
u	Instantaneous velocity in X-direction
$\bar{u}$	Local mean velocity in X-direction
u'	Velocity fluctuation in X-direction
X	Cartesian coordinate in longitudinal direction
Y	Cartesian coordinate in direction perpendicular to wind tunnel floor
Z	Cartesian coordinate in lateral direction
θ_s	Separation angle
μ	Dynamic viscosity of fluid
ν	Kinematic viscosity of fluid, μ/ρ
ρ	Density of fluid

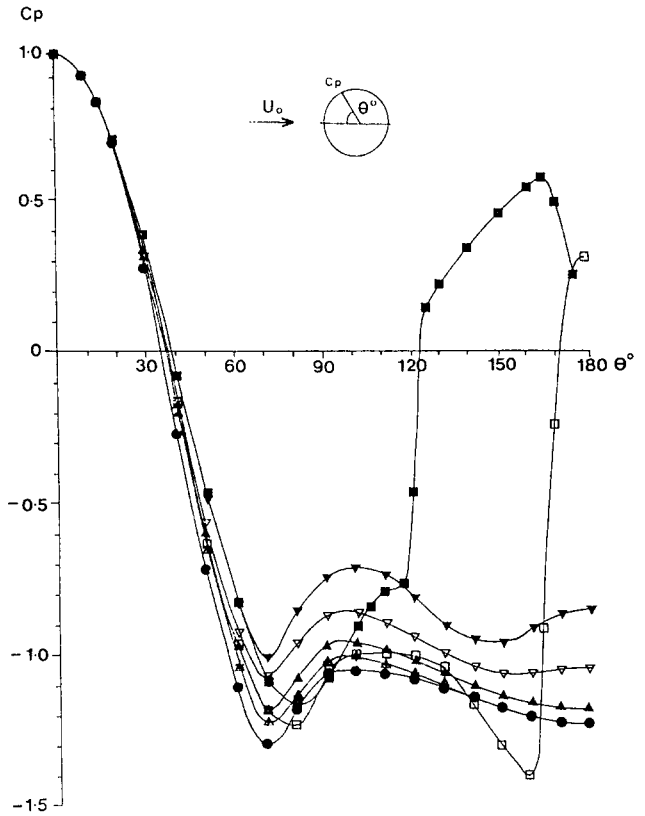

Figure 3 Circumferential pressure distributions around the centerline ($Y=0D$) of the upstream tube for spacings in the range $1 \leqslant L/D \leqslant 10$: ■, 1; □, 1.5; ▼, 2; ▽, 2.5; ▲, 3; △, 4; +, 5; ○, 10

Each separate hot wire system was connected via a 10-bit A/D converter to the microcomputer, which performed data acquisition and analysis.

The spatial correlation coefficient was calculated in accordance with the expression

$$R_u = \frac{\overline{u_1' \times u_2'}}{\sqrt{\overline{u_1'^2}} \times \sqrt{\overline{u_2'^2}}}$$

where u_1' and u_2' are the instantaneous u-component velocity fluctuations measured simultaneously at two separate points in the flow field (10,000 samples of both u_1' and u_2' were taken at each measurement position).

In addition to determining the streamwise spatial correlation, $R_u(X)$, the spanwise correlation, $R_u(Z)$, was also obtained in the immediate wake of the downstream tube. This enabled calculation of the integral length scale of turbulence in the Z-direction, L_{uz}, which denotes the spanwise magnitude of the turbulent eddy in the fluid motion at the stationary wire position and is defined as

$$L_{uz} = \int_0^z R_u(Z)\,\mathrm{d}z$$

The integral was evaluated by numerical integration of the spatial correlation curves, the upper limit, z, being taken as the location at which $R_u(Z)$ became zero.

Discussion of results

All of the tests described in this paper were carried out at a Reynolds number of $\mathrm{Re} = 2 \times 10^4$, based on a section diameter of 30 mm and a free-stream velocity of 10 m/s. This value is in the upper subcritical range for a circular cylinder and is compatible with previous work performed in this field. Measurements were made for a range of tube spacings varying from elements in contact, $L = 1D$, to a separation of 10 diameters, $L = 10D$, where L is defined as the distance between the central axis of each tube, Figure 2. The results of these experiments are discussed in detail below and, in addition, some comments are made on the possible heat transfer implications of this work.

The circumferential pressure distributions measured on the centerline of the upstream tube for the range of spacings investigated are presented in Figure 3, together with the corresponding distribution associated with a single tube. When the elements are in contact at the center of the configuration, $L = 1D$, the profile displays a unique curve which resembles that found by Zdravkovich[9] in experiments using high-blockage-ratio cylinders to form a similar geometry. The result obtained in the current work shows that a laminar boundary layer develops on the surface of the tube and is accelerated over the front face to an angle of approximately 80°. Beyond this point deceleration takes place and eventually transition to turbulence occurs within the attached flow, as indicated by the slight plateau in the distribution at about 110°. The turbulent boundary layer separates from the surface at approximately 125° and then reattaches at the rear of the tube in proximity to the point of contact. This latter phenomenon suggests that a small separation/reattachment "bubble" is established adjacent to the surface of the tube, a feature compatible with the results of oil film visualization experiments performed by Zdravkovich.[9] In the latter work, photographs of the flow pattern at the surface of the cylinders revealed the presence of a recirculation bubble which forms an arch in the spanwise direction, as illustrated in Figure 4.

As the distance between the two tubes is increased the recirculation bubbles, which are formed symmetrically on either side of the upstream tube, migrate over the surface, and become established in the gap created at the center of the geometry. This is evident in the circumferential pressure distribution measured at a member spacing of two diameters, $L = 2D$ (Figure 3), which displays a post-separation profile indicative of the presence of a recirculation "cell" in the wake of the upstream tube and in velocity measurements made with the pulsed wire anemometer.

The mean velocity and turbulence intensity profiles measured in the X-Z plane at the center of the gap for a tube spacing of two diameters, $L = 2D$, are shown in Figure 5(a) and (b), respectively. The shape of the velocity profile confirms the presence of these recirculation cells in the wake of the upstream tube. In this respect a considerable flow reversal occurs at the centerline of the wake, where a negative velocity was recorded with a value of 80% of that associated with the free-stream velocity, U_0. The point of zero velocity, which can be regarded as a guide to the position of the vortex center, is located at approximately $Z = 0.4D$, and the corresponding turbulence intensities, Figure 5(b), reach a peak value of 0.15 near the same position. The turbulence level falls rapidly in the Z-direction away from the vortex center to almost zero by $Z = 0.7D$, thus indicating the extent of the recirculation region.

Similar recirculation cells have been identified in experimental work by Kostic and Oka[3], and Ishigai *et al.*,[14] on the effect of member spacing upon the vortex shedding process associated with parallel cylinders arranged in tandem. In these experiments it was found that when the separation distance is small, $L < 3.8D$, a "closed wake" flow pattern

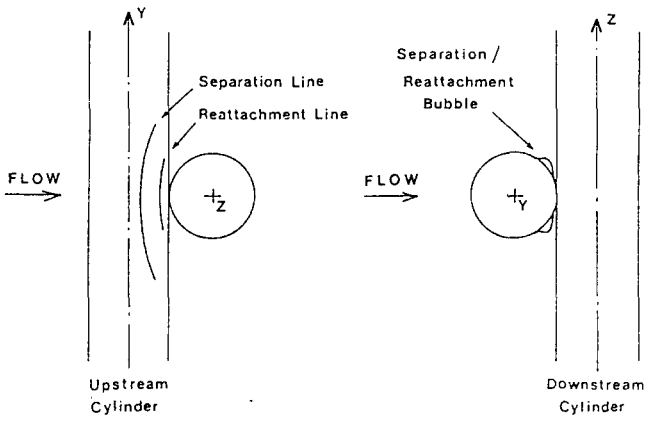

Figure 4 Sketch of separation/reattachment bubble at the center of the cross configuration (based on Zdravkovich[9])

composed of two counter rotating recirculation cells is formed within the gap between the two parallel cylinders. However, in the case of the perpendicular tubes examined in this study, the vortices do not persist in the spanwise direction of the upstream tube (*Y*-coordinate) as the constraint of the downstream element is not present beyond the center of the configuration.

The second flow regime in the gap commences at a separation distance of three diameters, $L=3D$, when the spacing of the members is sufficiently large to cause the recirculation cells to become unstable in the streamwise direction (X-coordinate). The corresponding pressure profile measured on the upstream tube, Figure 3, displays characteristics similar to those found on the surface of a single element and, therefore, suggests an equivalent flow regime. In this respect, a laminar boundary layer extends from the stagnation point through about 88° before separation, and the resulting free shear layers from either side of the cylinder form vortices which are shed in the gap. At this tube spacing the process in the wake of the central portion of the upstream tube is similar to that described by Gerrard[15] as occurring in the wake of a single cylinder in the subcritical Reynolds number range. Indeed, increasing the separation distance beyond three diameters, $L>3D$, results in a series of pressure profiles which tend towards the distribution measured on a single tube (Figure 3).

Further evidence for the onset of vortex shedding at the center of the upstream tube is clearly seen in the velocity profiles measured in the gap between the two tubes at a spacing of three diameters, $L=3D$. These are presented in Figure 6(a), together with the corresponding profiles obtained in the wake of a single tube. At each measurement position the velocities recorded in the gap are not exactly equivalent to those associated with the single tube, but they do exhibit a close approximation, particularly in the vortex formation region at one diameter downstream, $X=-2D$.

The corresponding turbulence intensity measurements presented in Figure 6(b) also indicate that the fluid motion in the wake of the upstream element is similar to that at the rear of a single tube. However, the turbulence levels associated with vortex shedding from the upstream tube are slightly higher at locations immediately downstream of the member, for example, the peak intensity measured at $X=-2D$ is increased by 13%, whereas the differences at $X=-1D$ are insignificant.

This relationship between vortex shedding and member spacing is again analogous to the phenomenon identified in experiments involving two parallel cylinders arranged in tandem. Observations by several workers, including Ishigai *et al.*,[14] Zdravkovich,[16] and Oka *et al.*,[17] established that vortex shedding commences in the wake of the upstream cylinder at spacings in excess of a critical value, $L>3.8D$. Kostic and Oka[3] explained this phenomenon by suggesting that shedding occurs when the size of the gap between the two cylinders is in excess of the size of the vortex formation region associated with a single cylinder. In the case of the current study, the size of the vortex formation region in the wake of the single tube can be considered as two and a half diameters (Bloor[18]). Hence, when the member spacing is three diameters, $L=3D$, the downstream tube is beyond this region.

These changes to the flow regime in the gap between the perpendicular tubes have a significant effect upon the airflow around the central portion of the downstream element. The lateral extent of this effect can be assessed by an examination of the spanwise distributions of stagnation pressure presented in Figure 7. These reveal that, regardless of member spacing, the interference to the flow conditions is largely confined to a region within two and a half diameters of the centerline of the downstream span, $Z\leqslant 2.5D$. In this respect, the stagnation pressures in the undisturbed outer region have values equivalent to those found at corresponding locations on a single tube, whereas those within the inner region are reduced to a minimum at the center of the span.

The nature of the disturbance to the flow conditions around the center of the downstream tube can be assessed by an examination of the circumferential pressure distributions shown in Figure 8. With the cylinders in contact at the center, $L=1D$, the curve exhibits a unique profile with negative coefficients recorded on the surface from the point of contact through

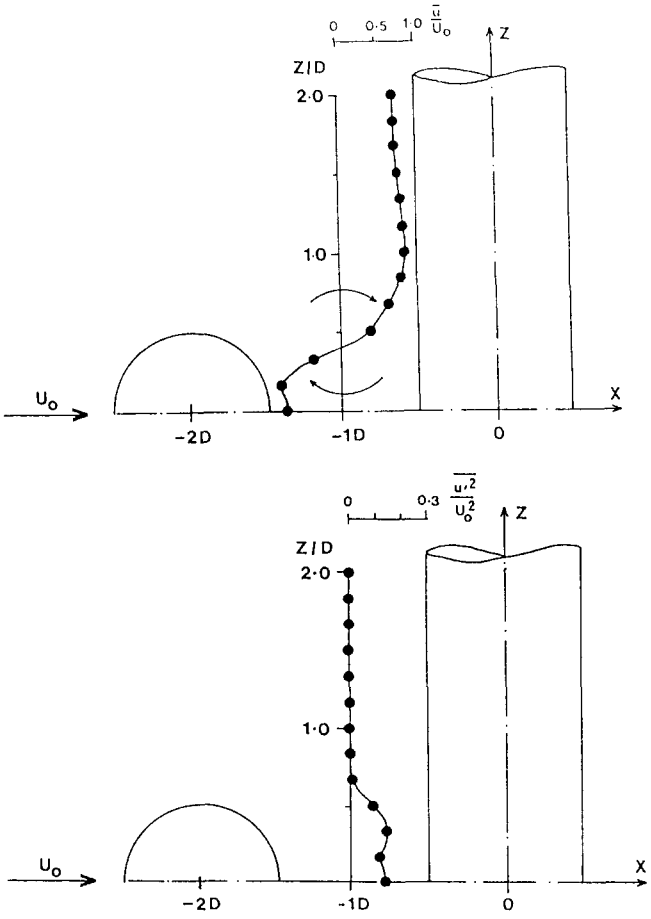

Figure 5 Mean velocity and turbulence intensity profiles recorded in the gap ($Y=0D$) between the perpendicular tubes for a spacing of $L=2D$: (a) velocity profiles; (b) turbulence intensities

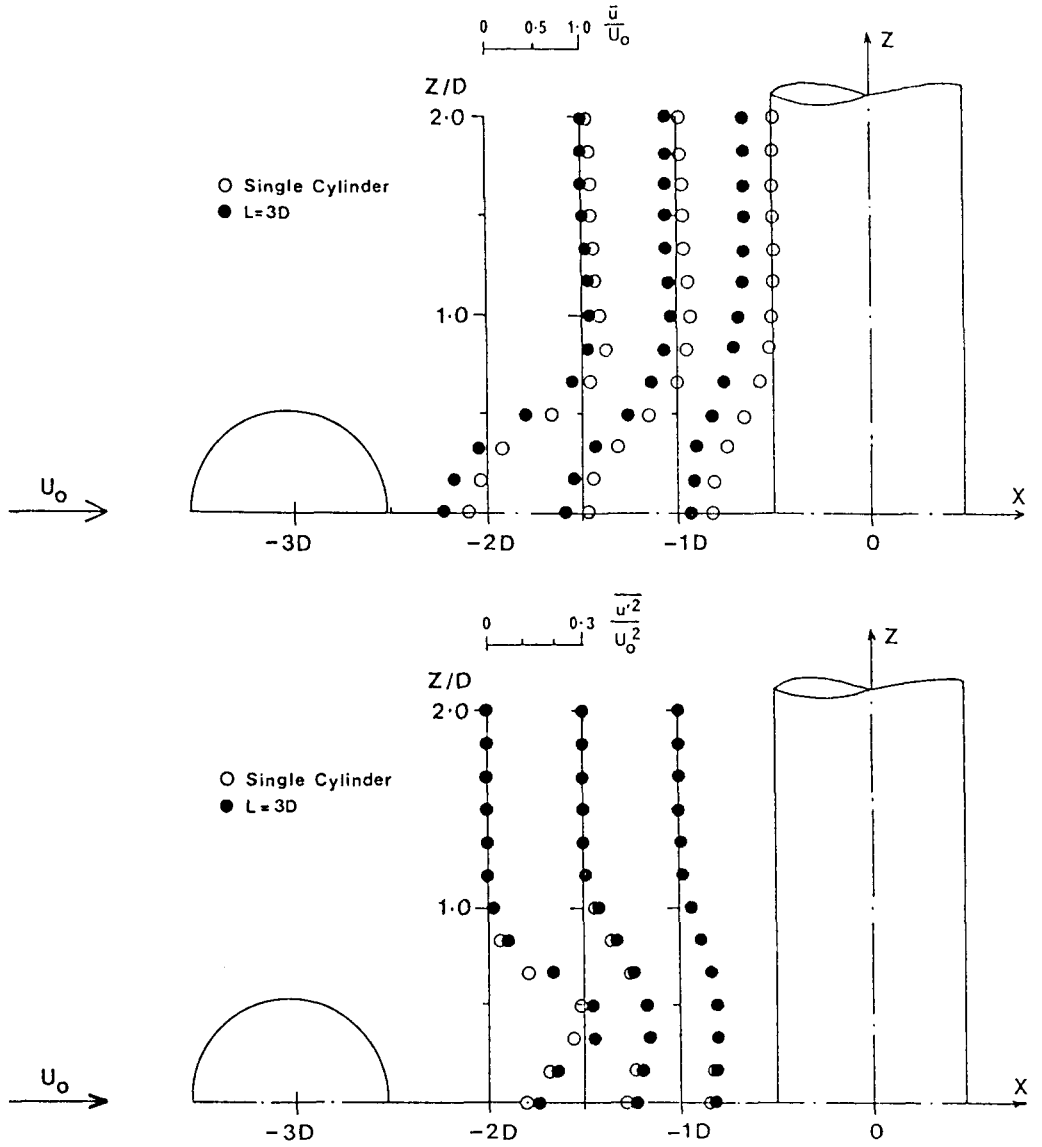

Figure 6 Mean velocity and turbulence intensity profiles recorded in the gap ($Y=0D$) between the perpendicular tubes for a spacing of $L=3D$: (a) velocity profiles; (b) turbulence intensities: ○, single cylinder; ●, $L=3D$

approximately 40°, a feature also noted in the experiments performed by Zdravkovich.[9] However, the introduction of a gap between the two tubes produces a family of curves for separation distances below three diameters, $L<3D$.

In this first range of spacings the profiles show that a boundary layer develops over the front face from a reduced stagnation pressure and separates at a point further downstream than on a single tube, as shown in Table 1. In addition, the post-separation sections of the curves show that there is considerable interference to the flow conditions at the rear surface of the tube, and that this causes a suppression of normal vortex shedding from the center of the span. The latter disturbance is particularly evident in the streamwise spatial correlation coefficients, $R_u(X)$, recorded in the wake (Figure 9). These show that at a separation distance below three diameters, $L<3D$, the coefficients associated with the fluid motion in the wake are uncorrelated with regard to the u-component in the X-direction.

At a spacing of three diameters, $L=3D$, a significant change occurs to the flow conditions in the gap with the establishment of streamwise vortex shedding from the central portion of the upstream tube. The effect of this second regime upon the airflow around the centerline of the downstream tube can be assessed from the circumferential pressure distributions presented in Figure 8. These show a decrease in the minimum value of pressure, C_p(min), and a post-separation profile similar to that found by Surry[19] on cylinders subjected to a turbulent approach flow. Indeed, the level of turbulence in the flow approaching the center of the downstream span is considerably higher than in the free-stream, as shown in the measurements presented in Figure 6(b). This increased turbulence results in a delayed separation at the surface of the tube and a narrower wake, the latter being evident as a rise in the base pressure on the rear of the tube, Figure 8. With increased gap widths beyond three diameters, $L>3D$, the pressure distributions continue to exhibit these features, and thus indicate that the turbulent wake generated by the upstream tube affects the center of the downstream span over the whole range of spacings observed.

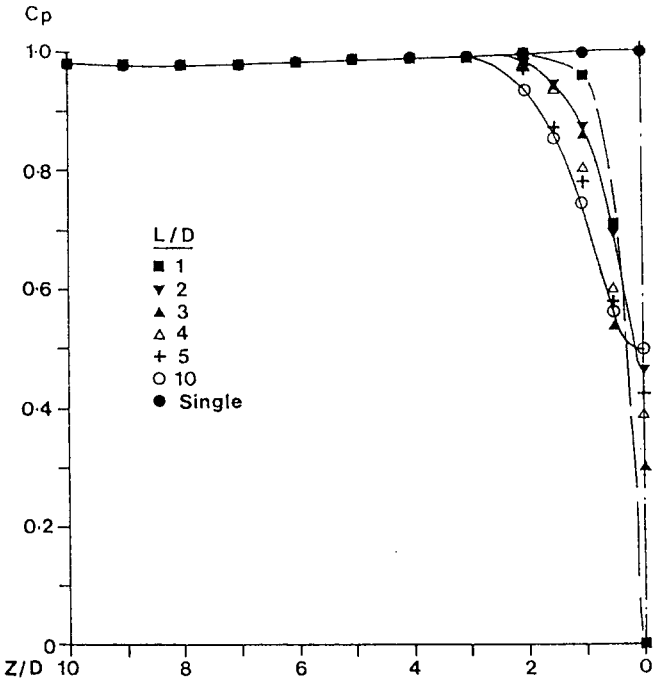

Figure 7 Spanwise stagnation pressure distributions on the downstream tube for spacings in the range $1 \leqslant L/D < 10$

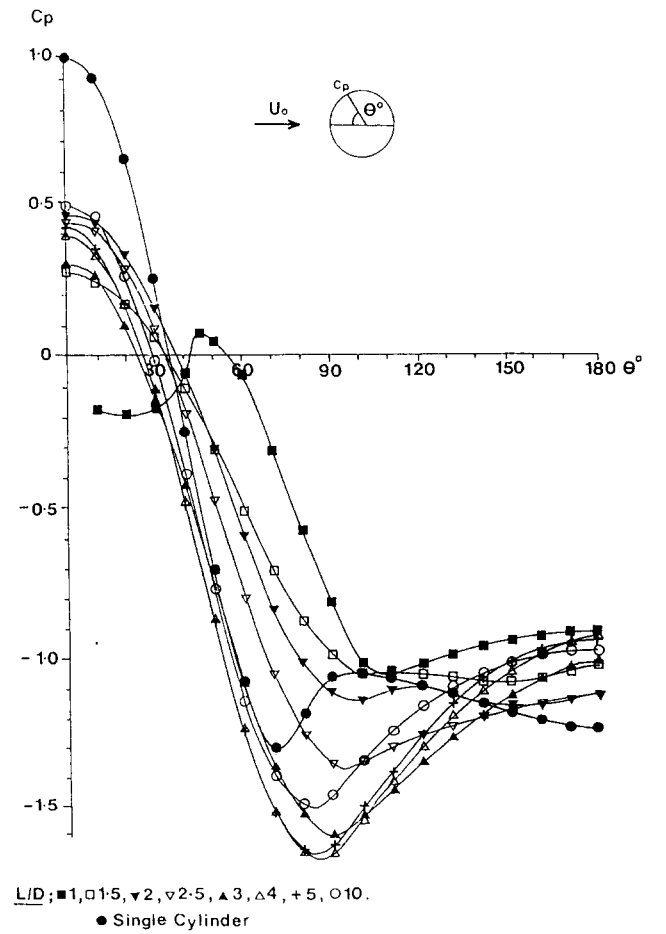

Figure 8 Circumferential pressure distributions around the centerline ($Z=0D$) of the downstream tube for spacings in the range $1 \leqslant L/D \leqslant 10$: ■, 1; □, 1.5; ▼, 2; ▽, 2.5; ▲, 3; △, 4; +, 5; ○, 10

To examine in more detail the variation with tube spacing of the turbulence levels in the approach flow to the downstream tube, turbulence intensity profiles were recorded in the X-Y plane at a location one diameter upstream of the centerline of the element, $X=-1D$. From the results of each traverse the maximum value of the turbulence intensity was evaluated, and these are presented in Table 2. Observation of the latter reveals that the turbulence level in the approach flow to the central portion of the downstream tube is in excess of the free-stream value throughout the range of spacings examined. For example, at a separation distance of three diameters, $L=3D$, the intensity is increased by a factor of 80. However, as the member spacing increases, the turbulence level shows a steady decrease, and the value is reduced to 20 times the free-stream when the separation distance is 10 diameters, $L=10D$.

Since the turbulence level in the gap decreases with increasing spacing, the degree of disturbance to the vortex shedding process associated with the downstream tube also decreases. This is reflected in the streamwise spatial correlations, $R_u(X)$, presented in Figure 9. These show that at a large spacing, for example, 15 diameters, $L=15D$, the fluid motion in the wake of the downstream tube exhibits a correlation which is similar in character to the curve associated with a single element. In this respect both correlations display periodicity in the variation of the coefficient, and the positions of the peak positive and negative values approximately coincide. However, despite this similarity, the disturbance to the shedding process in the wake of the downstream tube is apparent in the reduction of the coefficients in comparison with single tube values at each streamwise location. This decrease shows that the vortices shed from the downstream tube are highly turbulent and decay rapidly in the streamwise direction.

The corresponding changes in the spanwise extent of the turbulent eddy as a result of variations in tube spacing can be assessed by examining the Z-direction spatial correlations, $R_u(Z)$, recorded two diameters downstream of the tube (Figure 10). The coefficients presented for a separation distance of 15 diameters, $L=15D$, reveal that the disturbance to the flow conditions around the downstream tube reduces the spanwise correlation recorded in the wake relative to that associated with a single tube. This is evident as a rapid decrease of the coefficient to zero within two and a half diameters of the centerline, $Z=2.5D$, compared with six diameters for the single tube in uniform flow. Consequently, the value of the length scale, L_{uz}, calculated from the correlation is considerably reduced, as shown in Table 3, and the lateral size of the turbulent eddy is, therefore, much smaller than the equivalent shed by the single tube. The increase in the level of disturbance with decreasing separation distance results in a further reduction in the size of the eddy, and at spacings below three diameters, $L<3D$, the length scale, L_{uz}, decreases to practically zero.

Heat transfer implications

The results discussed above have shown that the flow regimes at the center of the cross are dependent upon tube spacing, and

Table 1 Variation of the separation angle at the center of the downstream span for tube spacings in the range $L<3D$

Tube spacing (L/D)	Separation angle $\theta°$
1.5	104°
2	116°
2.5	130°
single tube	88°

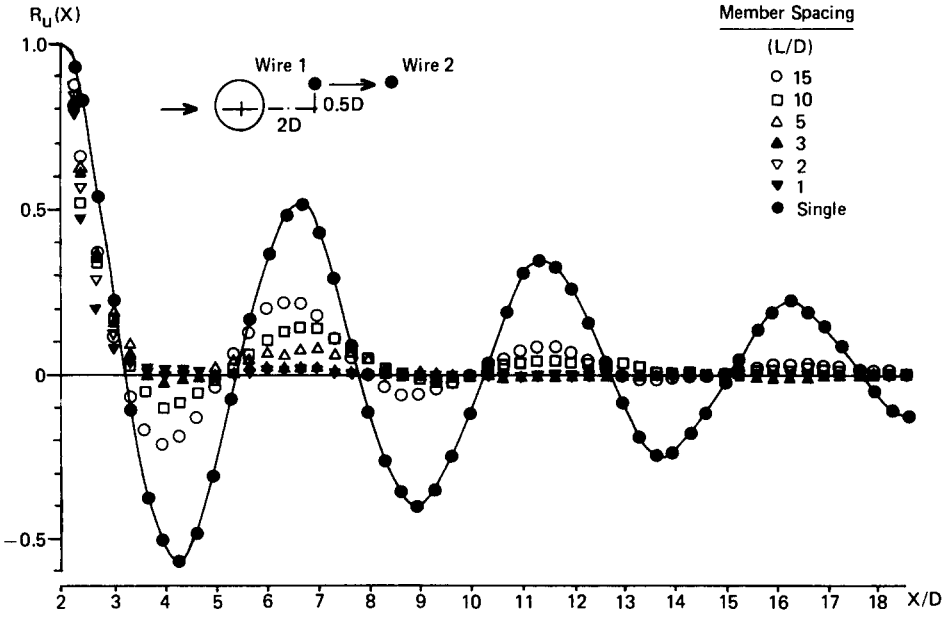

Figure 9 Streamwise spatial correlations recorded in the wake ($Z=0D$) of the downstream tube for spacings in the range $1 \leqslant L/D \leqslant 15$

Table 2 Maximum value of turbulence intensity in the approach flow to the downstream tube for spacings in the range $L \geqslant 3D$

Tube spacing (L/D)	Turbulence intensity at $X=-1D[\overline{u'^2}/U_0^2$ (max)]
3	0.141
4	0.076
5	0.064
10	0.037
free stream	0.0017

that they cause a considerable interference to the airflow around the central portion of the downstream tube. This disturbance was found to be limited to a spanwise region within two and a half diameters of the centerline of the configuration. Some comments are now made with regard to the possible implications of these findings for heat transfer rates at the surface of the downstream tube.

For tube spacings below three diameters, $L<3D$, it has been shown that a pair of symmetrical recirculation cells form in the gap at the center of the cross. These affect the flow conditions around the centerline of the downstream tube, resulting in a delayed separation point and thus an extension of the region of attached flow. This mechanism may lead to enhanced heat transfer rates at the surface of the tube as described in the case of parallel cylinders by Kostic and Oka.[3] However, beyond separation a gross disturbance to the vortex shedding process occurs, and consequently the contribution to the heat transfer capability of the fluid may be reduced in this second region relative to the single tube case. It is, therefore, difficult to estimate from these results alone whether there will be a net increase in heat transfer at the center of the span.

For an increase in tube spacing to three diameters and above, $L \geqslant 3D$, it was found that the central portion of the downstream span is subjected to the turbulent wake of the upstream element. This causes a transition of the surface boundary layer from laminar to turbulent, a delayed separation, and turbulent vortex shedding. It is therefore anticipated that in this case the heat transfer rates in the disturbed region will show a net increase relative to the rest of the tube. In addition, Kostic and Oka[3] identified local minimum heat transfer rates at the transition and separation points on the surface of a cylinder which may also be assumed to apply in this geometry.

The disturbance to the flow conditions at the surface of the downstream tube caused by the turbulence in the gap appears to be reduced as the distance between the tubes increases. It is therefore suggested that the associated heat transfer rates at the center of the span will also decrease relative to those recorded at lower tube spacings. However, the results corresponding to a gap width of 10 diameters indicate that for quite large spacings the central portion of the span may continue to exhibit heat transfer rates in excess of those associated with the rest of the tube.

Concluding remarks

The results of these experiments have provided general details of the flow conditions occurring in the gap at the center of a cross geometry composed of tubes. Two fundamental regimes were found which are dependent upon the tube spacing. At separation distances less than three diameters, $L<3D$, two recirculation cells are created in the wake of the upstream tube at the center of the span, and at larger spacings, when $L>3D$, these become unstable and are replaced by vortices which are shed in the direction of the free-stream.

These two regimes cause a significant disturbance to the flow conditions around the downstream tube, the spanwise extent of the interference effects being confined to a region within two and a half diameters of the centerline of the span. It has been suggested that this disturbance may lead to enhanced heat transfer rates at the surface of the tube, particularly when the central portion is positioned within the turbulent wake created by the upstream member at spacings beyond three diameters.

Although this paper has commented on the possible effects of

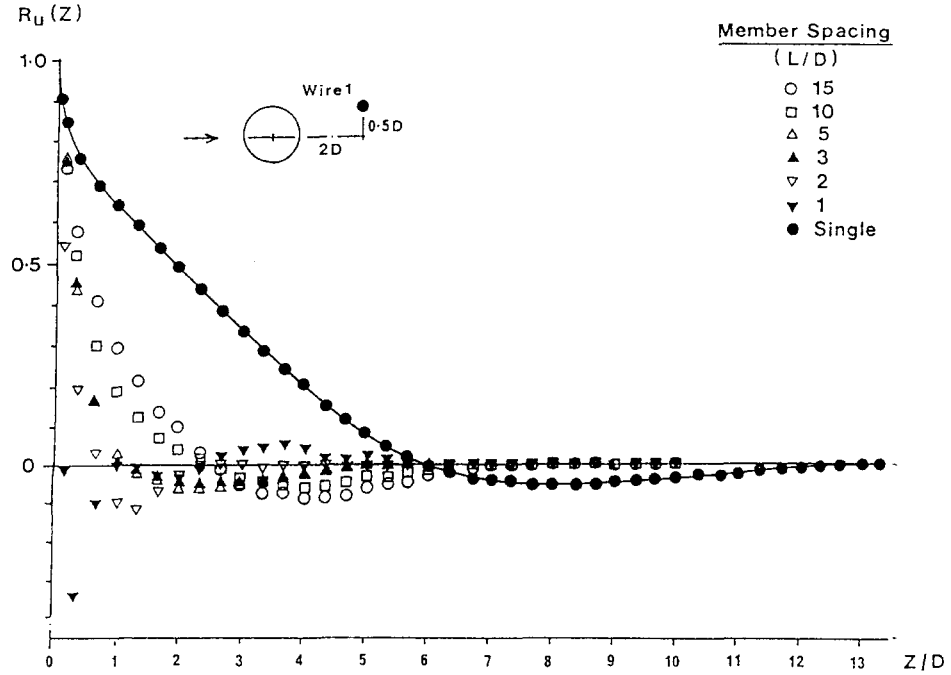

Figure 10 Spanwise spatial correlations recorded in the wake of the downstream tube for spacings in the range $1 \leqslant L/D \leqslant 15$

Table 3 Turbulence length scale, L_{uz}, recorded in the wake at the center of the downstream span

Tube spacing (L/D)	Length scale (L_{uz})
15	0.56D
10	0.46D
5	0.27D
3	0.26D
2	0.19D
1	0.09D
single tube	2.09D

All values determined with a fixed wire position of $X=2D$, $Y=0.5D$, $Z=0D$.

these flow regimes upon the heat transfer characteristics associated with the downstream tube, the work is far from complete. The next logical step would be to determine, by experiment, the actual variation of the heat transfer rates in an attempt to identify a maximum value that may occur at a critical spacing, and to evaluate the lateral extent of such an increase. This would provide details of the optimum tube and node spacing for the design of heat exchangers composed of perpendicular tubes.

Acknowledgment

The work described in this paper was funded through an S.E.R.C. Studentship awarded to T. A. Fox.

References

1 Van der Hegge Zijnen, B. G. Heat transfer from horizontal cylinders to a turbulent airflow. *Appl. Sci. Res.*, 1958, **7(A)**, 205–223

2 Zdravkovich, M. M. Review of flow interference between two circular cylinders in various arrangements. *Trans. ASME*, 1977, **99(I)**, 618–633

3 Kostic, Z. G. and Oka, S. N. Fluid flow and heat transfer with two cylinders in cross flow. *Int. J. Heat Mass Transfer*, 1972, **15**, 279–299

4 Hooper, J. D. and Rehme, K. Large scale effects in developed turbulent flow through closely spaced rod arrays. *J. Fluid Mech.*, 1984, **145**, 305–337

5 Osaka, H., Nakamura, I., Yamada, H., Kuwata, Y., and Kageyama, Y. The structure of a turbulent wake behind a cruciform circular cylinder. Part 1: the mean velocity field. *Bull. Japan Soc. Mech. Engrs.*, 1983, **26**, 356–363

6 Osaka, H., Yamada, H., Nakamura, I., Kuwata, Y., and Kageyama, Y. The structure of a turbulent wake behind a cruciform circular cylinder. Part 2: the streamwise development of turbulent flow fields. *Bull. Japan Soc. Mech. Engrs.*, 1983, **26**, 521–528

7 Osaka, H., Yamada, H., and Nakamura, I. Statistical characteristics of the turbulent wake behind intersecting cruciform circular cylinder. Proc. Fourth Symp. Turbulent Shear Flow, 1983, 5.37–5.47

8 Zdravkovich, M. M. Flow around two intersecting circular cylinders. *J. Fluid Eng. Trans ASME I*, 1985, **107**, 507–511

9 Zdravkovich, M. M. Interference between two circular cylinders forming a cross. *J. Fluid Mech.*, 1983, **128**, 231–246

10 E.S.D.U. Mean forces, pressures and flow field velocities for circular cylindrical structures: single cylinder with two-dimensional flow. Eng. Sci. Data Unit., 1980, 80025

11 E.S.D.U. Blockage corrections for bluff bodies in confined flows. Eng. Sci. Data Unit., 1980, 80024

12 Savory, E. and Toy, N. Microcomputer control of wind tunnel instrumentation with on-line data acquisition and analysis. *Software and Microsystems*, 1984, **3**, 93–97

13 Bradbury, L. J. S. and Castro, I. P. A pulsed wire technique for measurements in highly turbulent flows. *J. Fluid Mech.*, 1971, **49**, 657–691

14 Ishigai, S., Nishikawa, E., Nishimura, K., and Cho, K. Experimental study on structure of gas flow in tube banks with axis normal to flow. Part 1: Karman vortex flow around two tubes at various spacings. *Bull. Japan Soc. Mech. Engrs.*, 1972, **15**, 949–956

15 Gerrard, J. H. The mechanism of the formation region of vortices

behind bluff bodies. *J. Fluid Mech.*, 1966, **25**, 401–413
16 Zdravkovich, M. M. Smoke observations of wakes of tandem cylinders at low Reynolds numbers. *Aero. J.*, 1972, **76**, 108–114
17 Oka, S., Kostic, Z. G., and Sikmanovic, S. Investigation of the heat transfer process in tube banks in cross flow. Int. Sem. Recent Dev. in Heat Exchangers, 1972, Yugoslavia
18 Bloor, S. M. Transition to turbulence in the wake of a circular cylinder. *J. Fluid Mech.*, 1964, **19**, 290–304
19 Surry, D. Some effects of intense turbulence on the aerodynamics of a circular cylinder at subcritical Reynolds number. *J. Fluid Mech.*, 1972, **52**, 543–563